Considering the effect of killing time on the density of oxides, Ueshima *et al.*[13] reported that the shortening of the killing time led to an increase in the density of Ti oxides. The present study shows the same trend. The reasonable interpretation may be that prolonging the holding time before casting allows the Ti oxide that has formed at the early stage to grow and float up, thereby reducing the density of Ti oxide in steel plate. This proposal can be supported threefold: (1) the oxygen level in molten state (about 45 ppm) is higher than that in steel plate (Table I), (2) steel T2 has higher oxygen content than steel T1 due to its shorter holding time before casting, and (3) steel T2 has more uneven distribution of inclusions because of its lack of time to allow larger inclusions to float up.

In summary, the timing of Ti killing had an effect on the chemistry of inclusions. This, in turn, affected the microstructure and the toughness of the HAZ. Reducing the duration between Ti killing and casting resulted in a higher density of TiO-dominant inclusions, which led to a higher volume fraction of intragranular ferrite in the microstructure and a better toughness of the HAZ.

The authors are grateful to China Steel Corporation for permission to publish this note.

REFERENCES

1. J. Furusawa, K. Arimochi, H. Kurayasu, N. Nakano, and S. Suzuki: *Sumitomo Kinzoku*, 1988, vol. 40, pp. 39-47.
2. S. Deshimaru, I. Hirai, K. Amano, S. Ueda, T. Uemura, and K. Tsubota: Kawasaki Steel Technical Report No. 17, 1987, pp. 34-40.
3. F. Heisterkamp, K. Hulka, and A.D. Batte: in *Int. Conf. on The Metallurgy, Welding and Qualification of Microalloyed HSLA Steel Weldments*, American Welding Society, Houston, TX, 1990, pp. 638-60.
4. S. Ohkita, M. Wakabayashi, H. Homma, K. Yamamoto, and S. Matsuda: Nippon Steel Technical Report No. 37, 1988, pp. 10-16.
5. M. Koibe, H. Honma, S. Matsuda, M. Imagunbai, M. Hirai, and F. Yamaguchi: U.S. Patent 4629504, Dec. 16, 1986.
6. K. Yamamoto, S. Matsuda, T. Haze, R. Chijiiwa, and H. Mimura: in *Residual and Unspecified Elements in Steel*, ASTM STP 1042, A.S. Melilli and E.G. Nisbett, eds., 1989, pp. 264-84.
7. J.L. Lee and Y.T. Pan: *Mater. Sci. Eng.*, 1991, vol. A136, pp. 109-19.
8. H.K.D.H. Bhadeshia: in *Int. Conf. on The Metallurgy, Welding and Qualification of Microalloyed HSLA Steel Weldments*, American Welding Society, Houston, TX, 1990, pp. 34-69.
9. J. Jang and J.E. Indacochea: *J. Mater. Sci.*, 1987, vol. 22, pp. 689-700.
10. F.J. Barbaro, P. Krauklis, and K.E. Easterling: *Mater. Sci. Technol.*, 1989, vol. 5, pp. 1057-68.
11. R.A. Ricks, P.R. Howell, and G.S. Barrihle: *J. Mater. Sci.*, 1982, vol. 17, pp. 732-40.
12. S. Kanazawa, A. Nakashima, K. Okamoto, and K. Kanaya: *Tetsu-to-Hagané*, 1975, vol. 11, pp. 65-79.
13. Y. Usehima, H. Yuyama, S. Mizoguchi, and H. Kajioka: *Tetsue-to-Hagané*, 1989, vol. 75, pp. 123-30.

Effect of Plastic Deformation on Residual Stresses in Ceramic/Metal Interfaces

YUNHONG ZHOU, KENJI IKEUCHI, THOMAS H. NORTH, and ZHIRUI WANG

Considerable effort has been made to develop interlayer materials which minimize the residual stresses produced by thermal expansion mismatch during ceramic/metal joining. In spite of previous studies, it is still not clear which combination of factors controls interlayer selection.

Naka *et al.*[1] examined the joining of Si_3N_4 to other ceramics, such as alumina and zirconia, and to metal substrates, such as Fe, Cu, Invar, Kovar, and AISI stainless steel, using amorphous Cu-Ti filler metal and concluded that tensile strength of the joint decreased as the difference in thermal expansivities of the ceramic and the metal substrate increased. Also, the tensile strength of ceramic/metal joints decreased as the product of the thermal expansivity and the elastic modulus of the metal substrate increased. Nicholas and Crispin[2] also found a clear relation between final joint strength and increasing thermal expansivity mismatch during diffusion bonding of alumina to different metal substrates. These results were explained on the basis that high thermal mismatch stresses facilitated joint failure at low applied loads. Based on these results, the interlayer material should have a thermal expansivity as close as possible to that of the ceramics being joined.

On the other hand, when a relatively thick interlayer material was placed between the ceramic and metal substrates, Zhou *et al.*[3] and Hamada *et al.*[4] found a relation which appears to be quite the opposite, namely, that increasing thermal expansivity mismatch was associated with higher joint strength. These results were explained on the basis that the interlayer material yielded during cooling after brazing, and that this relaxed the thermal stresses produced at the ceramic/metal interface. These results suggest that the use of low yield strength/high ductility interlayer materials is the most effective method of improving final joint strength.

In the present work, the effect of interlayer plastic deformation on the residual stress is studied using a revised simple model of ceramic/metal joint.

The interplay between thermal mismatch stresses and interlayer plastic deformation is easily illustrated using a one-dimensional model of the ceramic/metal joining operation, *i.e.*, two parallel rods, the metal rod I and the ceramic rod II, of the same length and cross-sectional areas are fixed at one end and are restrained to move together at their other end (Figure 1). In this case, it is assumed that the displacement only occurs parallel to the

---

YUNHONG ZHOU, Graduate Student, THOMAS H. NORTH, Associate Professor, and ZHIRUI WANG, Assistant Professor, are with the Department of Metallurgy and Materials Science, University of Toronto, Toronto, ON M5S 1A4, Canada. KENJI IKEUCHI, Associate Professor, is with the Welding Research Institute, Osaka University, Osaka 567, Japan.

Manuscript submitted February 6, 1991.

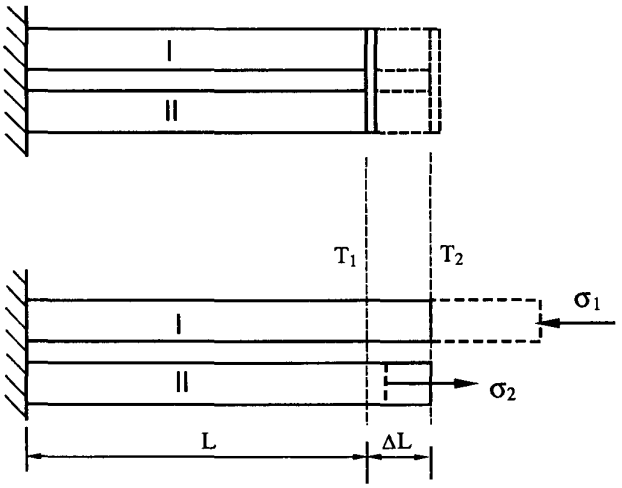

Fig. 1—One-dimensional model for ceramic/metal joint (the metal rod is I and the ceramic rod is II; temperature changes from T_1 to T_2).

rod axes, and the thermal stress generated in the joint by a given temperature change is given by the well-known relation

$$\sigma = \Delta\alpha\Delta T \frac{E_I E_{II}}{E_I + E_{II}} \quad [1]$$

where $\Delta\alpha = \alpha_I - \alpha_{II}$ and α_I and α_{II} are the thermal expansivities of the metal and ceramic rods, respectively, $\Delta T = T_2 - T_1$ is the temperature change, and E_I and E_{II} are the elastic modulus of the metal and ceramic rods, respectively. However, this relation applies only when the thermal stress is lower than the yield stress of the metal rod. When the thermal stress in the metal rod exceeds its yield strength, the determining equation for the thermal stress should be changed, and the analysis is given as follows.

Assuming a linear elastic-linear plastic behavior of the metal rod (Figure 1), the thermal stress in the metal rod following yielding, σ_I, is given as

$$\sigma_I = \sigma_{IY} + E_{IP}\left(\varepsilon_I - \frac{\sigma_{IY}}{E_I}\right) \quad [2]$$

and therefore,

$$\varepsilon_I = \frac{\sigma_I - \sigma_{IY}}{E_{IP}} + \frac{\sigma_{IY}}{E_I} \quad [3]$$

where E_I and E_{IP} are the elastic modulus and linearly hardening coefficient of the metal rod, respectively, σ_{IY} is the yield strength, and ε_I is the strain in the metal rod.

The strain of the ceramic rod, ε_{II}, is

$$\varepsilon_{II} = \frac{\sigma_{II}}{E_{II}} \quad [4]$$

where σ_{II} and E_{II} are the thermal stress and elastic modulus in the ceramic rod, respectively. If the differential expansion of the two rods due to the change in temperature is accommodated by the deformations which occur in both materials, then the real elongation in both rods should be equal to each other, $\Delta L_I = \Delta L_{II}$, and therefore,

$$L\Delta T\alpha_I - L\varepsilon_I = L\Delta T\alpha_{II} + L\varepsilon_{II} \quad [5]$$

where L is the original length of the two rods, and α_I and α_{II} are the coefficients of thermal expansion of the two materials, respectively. Since both rods have the same cross-sectional area, then $\sigma_I = \sigma_{II} = \sigma$, the nominal thermal stress. Using Eqs. [3] through [5], one can obtain the following relation:

$$\sigma = \left(\Delta\alpha\Delta T + \frac{E_I - E_{IP}}{E_I E_{IP}}\sigma_{IY}\right)\frac{E_{II}E_{IP}}{E_{II} + E_{IP}} \quad [6]$$

Since $E_{IP} \ll E_I$ and also $E_{IP} \ll E_{II}$,

$$\sigma = \sigma_{IY} + E_{IP}\Delta\alpha\Delta T \quad [7]$$

It follows that the residual thermal stress in the rods is given by Eq. [1] when the stress in the joint is less than the yield stress of the metal rod and Eq. [7] when the stress is larger than the yield stress.

When a high yield strength metal is employed, the thermal stresses are determined by Eq. [1], and the thermal expansivity difference between the ceramic and the metal is obviously the critical factor. However, when metal yielding occurs, thermal stress depends on both the yield strength (σ_{IY}) and also the thermal strain term, $E_{IP}\Delta\alpha\Delta T$, but predominantly on the yield strength, because it is much larger than the second term in practice, as indicated by Eq. [7]. As an example, consider bonding between Si_3N_4 and two different materials, copper and molybdenum. The thermal stresses for the two cases can be calculated based upon Eqs. [1] and [7] with the data shown in Table I, and the results are shown in Figure 2. The linear hardening coefficient used in Eq. [7] is calculated from yield stress, tensile strength, and elongation. If the change in temperature is very small, the residual thermal stresses are dominated by thermal expansion mismatch, and Cu will have the highest thermal stress. On the other hand, when the change in temperature is large, the yield strength and the plastic deformation due to the thermal stress play a major role, leading to a very low residual stress in the Cu case and a high residual stress in the Mo case.

Table I. Physical and Mechanical Properties of Materials[5,6]

Materials	Young's Modulus (GPa)	Coefficient of Thermal Expansion (10^{-6}/K)	Mechanical Properties		
			0.2 Pct Yield Stress (MPa)	Tensile Strength (MPa)	Elongation (Pct)
Copper	129.8	17.0	48	216	48
Molybdenum	324.8	5.1	345	435	5 to 25
Si_3N_4	320	3.2	—	—	—

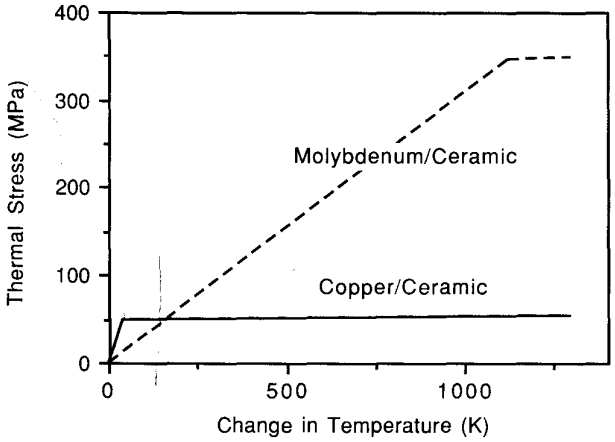

Fig. 2—Relationship between thermal stresses and temperature change for two ceramic/metal composites.

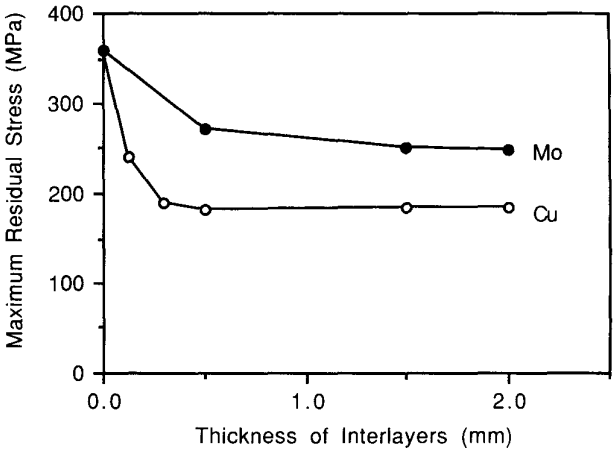

Fig. 3—Effect of interlayer thickness on the finite element method-calculated maximum residual stresses in Si_3N_4/steel joints when using copper and molybdenum interlayers.[13]

It is also important to point out that the actual ceramic/metal joints are more complicated (*e.g.*, the thermal stress situation is a three-dimensional problem, and the thermal stresses are produced during the cooling period after the joining operation, *etc.*). Therefore, Figure 2 can only be taken as an origin for a qualitative consideration. From the above discussion, it is apparent that interlayer yielding sometimes can play an important role in controlling the property of the joint. It follows that replacement of a ductile interlayer, such as copper, by another metal, which has a lower thermal expansivity but higher yield strength, may decrease final joint strength due to a restricted plastic flow and subsequent relaxation of thermal stresses. This effect has been observed during alumina/steel joining, when a copper interlayer was replaced by nickel and resulted in cracked joints.[4]

In addition to the above factors, it is also important to realize that the interlayer thickness and the mechanical properties of the metal substrate will strongly affect the yielding process. When a very thin copper interlayer is considered, the restraint induced by the difference in the elastic modulus and yield strength of the steel substrate and the copper interlayer will inhibit the yielding process. The restraint produced by a more rigid substrate induces triaxial stresses in the adhesive layer and increases the apparent elastic modulus and yield strength during adhesive bonding.[7] This effect has been used to explain why the tensile strength of low adhesive thickness joints is much higher than that of the bulk adhesive. If it is assumed that yielding of a thin copper interlayer during ceramic/metal joining is similarly affected by the mechanical properties of the metal substrate material, then the apparent yield strength and apparent elastic modulus value of the interlayer will be higher than expected. This means that the tensile strength of bulk copper material (measured using uniaxial testing) will be unrepresentative and much lower than that existing in the actual ceramic/metal joint.

When the thickness of the interlayer material increases, the restraint effect due to the metal substrate becomes less important. The results have confirmed that increasing Cu or Mo interlayer thickness decreases the finite element method-calculated thermal stresses produced in Si_3N_4/steel joints[3] (Figure 3). Increasing the Cu interlayer thickness has been associated with higher joint fracture strength when joining alumina to steel[4] and when joining alumina to steel using Al-Si interlayer materials.[8]

Figure 3 indicates that the maximum thermal stresses are lower when a copper interlayer is used, and that these reach a constancy when the thickness of the copper layer exceeds 0.5 mm. When a molybdenum interlayer is used instead of copper, the thermal stresses also reach a constancy when the insert thickness exceeds 1.5 mm. It follows that the elastic constraint due to the rigid steel substrate is also important when thin molybdenum interlayer is used. In fact, when the interlayer is thick enough, the stresses generated during ceramic/metal joining depend only on the properties of the interlayer and the ceramic material. The mechanical behavior of constrained interlayers is very complicated;[9] detailed work is needed to determine the relationship between the interlayer thickness and mechanical properties of the ceramic/metal joint.

In conclusion, the selection of interlayers for ceramic/metal joining must consider not only the difference in thermal expansion mismatch but also the influence of interlayer stress-strain characteristics and interlayer thickness. In practice, more attention should be paid to the important role of the interlayer's plastic deformation in relaxing the thermal stresses produced during joining operation.

REFERENCES

1. M. Naka, T. Tanaka, and I. Okamoto: *Trans. Jpn. Weld. Res. Inst.*, 1985, vol. 14, pp. 85-91.
2. M.G. Nicholas and R.M. Crispin: *J. Mater. Sci.*, 1982, vol. 17, pp. 3347-60.
3. Y. Zhou, F.H. Bao, J.L. Ren, and T.H. North: *Mater. Sci. Technol.*, 1991, in press.
4. K. Hamada, M. Kureishi, T. Enjo, and K. Ikeuchi: I.I.W. Doc. I-812-86/OE, 1986.

5. *Smithell's Metals Reference Book*, Butterworth's, London, 1983, 6th ed., pp. 14-1, 14-2, 15-2, 15-3, 22-23, and 22-190.
6. *ASM Engineered Materials Reference Book*, ASM, Metals Park, OH, 1989.
7. R.D. Adams and J. Coppendale: *J. Adhesion*, 1979, vol. 10, p. 49.
8. T. Yamada, K. Yokoi, and A. Kohno: *J. Mater. Sci.*, 1990, vol. 25, pp. 2188-92.
9. R.J. Klassen: Ph.D. Thesis, University of Toronto, Toronto, ON, Canada, 1990.

Measurements of Rapid Solidification Rate in Highly Undercooled Melts with a Video System

M. SUZUKI, T.J. PICCONE, and M.C. FLEMINGS

This article describes results of experiments using a video system for direct measurement of dendrite tip velocity in undercooled alloy melts and comparison of results with those obtained from optical temperature measurements and with calculations using a dendrite growth model based on the analysis by Boettinger *et al.*[1]

High-speed cinematography[2,3] and high-speed optical temperature measurement systems[4,5,6] have been used to measure dendrite tip velocity. The strong points of high-speed cinematography are its ability to measure relatively high solidification rates and the high resolution attainable on film. Wu *et al.*[3] measured tip velocities as high as 0.7 m/s in Ni-25 pct Sn alloy. Weak points of this method are the inability to observe results immediately and high cost.

In order to obtain an estimate of solidification rate using an optical temperature measuring device, it is necessary to calculate growth rate from recalescence time. It is not possible to observe growth morphology by this method.

The experimental apparatus used in this work consists of a high-frequency induction melter, a high-speed optical temperature measurement system, and a monochrome video system. The method for obtaining thermal histories using the high-speed temperature measurement system has been given elsewhere.[3,4] The video system consists of a Cliftondale Electronics model FT-450 monochrome video camera, a PANASONIC* model WV-5410 monitor, and a PANASONIC model AG-1830 video cassette recorder. The camera uses noninterlace scanning, and the recorder performs field-sequential playback, allowing the recording and observation of fields, rather than frames composed of two superimposed fields. The system provides 60 independent images per second.

*PANASONIC is a trademark of Matsushita Electric Corp. of America, Secaucus, NJ.

M. SUZUKI, Assistant Manager, is with the Material Research and Development Department, Toyota Motor Corporation, Toyota City, Japan. T.J. PICCONE, Postdoctoral Associate, and M.C. FLEMINGS, Professor and Department Head, are with the Department of Materials Science and Engineering, Massachusetts Institute of Technology, Cambridge, MA 02139.

Manuscript submitted September 26, 1990.

The video camera was set in the same horizontal plane as a dual-wavelength pyrometer. The angles between the pyrometer and the camera were 40 and 90 deg for 3.2 g spherical samples and 10 g rectangular samples, respectively. Actual magnification on the monitor is 17 times. Measurement of thermal history and recording of video images were conducted simultaneously. In order to obtain solidification rate (dendrite tip velocity) from video images, a sequence of images was traced, field by field, on a transparency sheet from the monitor, and the position of the interface corresponding to the thermal front was determined along approximately straight lines in the direction of motion as a function of time.

The Fe-2 wt pct B and Fe-6 wt pct P alloys were used. Samples were prepared by high-frequency induction melting of iron pieces (purity 99.98 pct) with either iron boride (Fe_2B) particles (purity 99 pct) or iron phosphide (Fe_2P) particles (purity 99.9 pct). The samples of iron-boron alloy, either 3.2 or 10 g in mass, were melted and solidified within molten B_2O_3 under argon atmosphere. Samples of iron-phosphorus alloy, 3.2 g in mass, were melted and solidified within borosilicate glass under argon atmosphere. B_2O_3 was used instead of borosilicate glass for iron-boron alloys to avoid reaction of boron with silica in the glass.

Figure 1 is a typical single field from a series of video images of a spherical Fe-2 wt pct B alloy sample undercooled 165 K. Figure 2 is a similar field for a rectangular Fe-2 wt pct B alloy sample undercooled 103 K. In these figures, the white area represents the solidifying portion, which is partially solid, and the dark area represents the remaining undercooled liquid. The white region has a higher average temperature than the dark region due to the release of heat of fusion accompanying solidification (recalescence).

The interface between the light and dark regions is a narrow thermal boundary layer with a steep temperature gradient. The actual dendrite tips must be within this boundary layer, although they are submicroscopic in size and cannot be resolved optically. The dendrite tips should be smaller in size than the observed tips of the thermal front by a factor equal to the ratio of the thermal and solute diffusion coefficients in the liquid phase. For metal

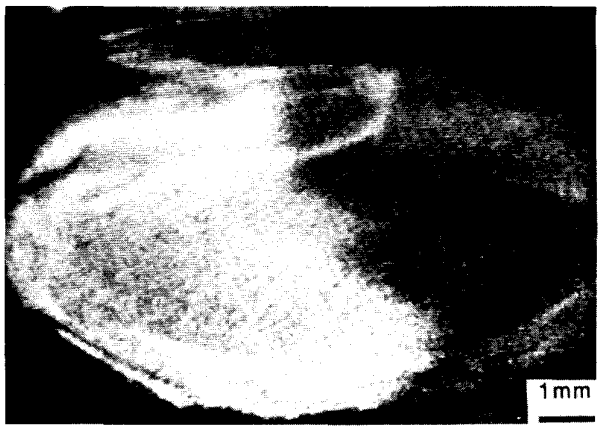

Fig. 1—Typical example of a single field obtained during recalescence of a spherical Fe-2 wt pct B alloy sample undercooled 165 K.